JOURNAL OF AGRICULTURAL AND FOOD CHEMISTRY

Detection of a "Nonaromatic" NIH Shift during In Vivo Metabolism of the Monoterpene Carvone in Humans

WOLFGANG ENGEL*

Deutsche Forschungsanstalt für Lebensmittelchemie, Lichtenbergstrasse 4, D-85748 Garching, Germany

High-resolution gas chromatography in combination with mass spectrometry and high-resolution mass spectrometry was used to determine the positions and extent of labeling in the metabolites of carvone, namely in α,4-dimethyl-5-oxo-3-cyclohexene-1-acetic acid (dihydrocarvonic acid), α-methylene-4-methyl-5-oxo-3-cyclohexene-1-acetic acid (carvonic acid), and 5-(1,2-dihydroxy-1-methylethyl)-2-methyl-2-cyclohexen-1-one (uroterpenolone), after human ingestion of 9,9-dideutero- and 9-^{13}C-carvone. Carvonic acid was formed by oxidation at the methyl carbon of the isopropenyl group of carvone, whereas dihydrocarvonic acid was formed by oxidation at the methylene position, most probably via carvone epoxide. A "nonaromatic" NIH shift must occur during the subsequent reactions yielding dihydrocarvonic acid. Additionally, dehydrogenation of dihydrocarvonic acid and hydrogenation of carvonic acid were observed, resulting in minor amounts of both acids owning a carboxy group of opposite origin. Uroterpenolone was found to be exclusively formed by oxidation at the methylene carbon of the isopropenyl group of carvone, and thus, most probably by hydrolysis of carvone epoxide.

KEYWORDS: MICA; urinary metabolites; α,4-dimethyl-5-oxo-3-cyclohexene-1-acetic acid; α-methylene-4-methyl-5-oxo-3-cyclohexene-1-acetic acid; 5-(1,2-dihydroxy-1-methylethyl)-2-methyl-2-cyclohexen-1-one; carvone; 9,9-dideutero-carvone; 9-(^{13}C)-carvone; nonaromatic NIH shift

INTRODUCTION

In a previous study (*1*) the following compounds were identified as the major oxygenated metabolites of carvone in humans using the metabolism of ingestion-correlated amounts (MICA) approach: α,4-dimethyl-5-oxo-3-cyclohexene-l-acetic acid (dihydrocarvonic acid, **M1**), α-methylene-4-methyl-5-oxo-3-cyclohexene-1-acetic acid (carvonic acid, **M2**), and 5-(1,2-dihydroxy-1-methylethyl)-2-methyl-2-cyclohexen-1-one (uroterpenolone, **M3**). However, the structures of the metabolites provided little information about the mechanisms by which they were generated, especially if the methyl or the methylene carbon of the isopropenyl group of carvone was oxidized. To our knowledge there are no studies reported in the literature in which labeling with stable or radioactive isotopes was performed to clarify the oxidation mechanism of the isopropenyl group of terpenes which occurs frequently, for example, in carvone, limonene, carveol, and many others.

Therefore, a MICA experiment using site-specifically labeled carvone should provide further valuable information about the in vivo metabolic pathways of carvone in humans and more generally of the isopropenyl group of terpenes. Additionally, in the previous study (*1*) the metabolites of carvone were identified only by comparison of control and test urine. Because of the very low amount of carvone applied, which is a prerequisite of a MICA experiment, contamination with other terpenes from the diet or cosmetics is difficult to rule out. Application of labeled carvone could conclusively prove the origin of the proposed metabolites by the presence of the incorporated label.

The aim of this study was, therefore, first to develop a synthetic method that would provide carvone labeled with stable isotopes, namely with deuterium and carbon 13, at relevant and distinct positions; and second, to deduce the metabolic pathways of carvone metabolism in MICA experiments in humans from the distribution and the position of the labels found in the known metabolites.

MATERIALS AND METHODS

Chemicals. Sodium metaperiodate was from Merck (Darmstadt, Germany), triphenylphosphine, D_3-iodomethane, ^{13}C-iodomethane, sodium hydride, and butyl lithium (2.5 mmol/mL in hexane) were from Aldrich (Steinheim, Germany).

MICA Experiment. Human experimentation was performed as previously described (*1*) except that only the author participated. The amount of terpene applied was 15 mg (0.2 mmol; 200 μg/kg body mass) of either 9,9-dideutero-carvone or 9-^{13}C-carvone.

Isolation of Metabolites from Urine and Derivatization Procedures. Isolation was performed as previously described (*1*). Briefly, after enzymatic hydrolysis at pH 5.0 with glucuronidase and sulfatase from *Helix pomatia* and acidification to pH 2.0 with concentrated HCl, the metabolites were extracted with diethyl ether. The metabolites in the acidic fraction were trimethylsilylated with BSTFA or ethylated with iodoethane (*1*).

* Author may be contacted by telephone 0049 (0)89 28914375, fax 0049 (0)89 28914183, or e-mail wolfy@dfa.leb.chemie.tu-muenchen.de.

10.1021/jf011199h CCC: $22.00 © 2002 American Chemical Society
Published on Web 02/14/2002

Purification of the Acidic Metabolites by High-Pressure Liquid Chromatography (HPLC). The ethylated mixture of the acidic metabolites was concentrated to about 50 μL and diluted with pentane to a total volume of 100 μL. HPLC separation was performed in a single run on a polar diol phase column (250 mm × 4.6 mm i. d.; Lichrospher 100 Diol, 5 μm, Merck, Darmstadt, Germany) using a pentane−diethyl ether gradient at a flow of 1 mL/min. The gradient started with pentane/diethyl ether 92:8, v/v, and was raised within 40 min to a final concentration of pentane/diethyl ether 12:88, v/v. Fractions were collected at 1-min. intervals, concentrated, and checked by HRGC−MS for the presence of the ethyl esters of **M1 (M1-ET**) or **M2** (**M2-ET**). Both acids were localized in the fraction eluting between 12 and 13 min.

Synthesis of 9,9-Dideutero-Carvone and 9-^{13}C-Carvone. *5-(1,2-dihydroxy-1-methylethyl)-2-methyl-2-cyclohexen-1-one.* The synthesis was performed as described earlier (*1*). Briefly, carvone was epoxygenated, and the epoxide was cleaved by H_2SO_4 in aqueous THF.

5-Acetyl-2-methyl-2-cyclohexen-1-one. To a stirred solution of 5-(1,2-dihydroxy-1-methylethyl)-2-methyl-2-cyclohexen-1-one (6.5 mmol, 1.2 g) in methanol (10 mL) and water (10 mL), a solution of sodium metaperiodate (6.5 mmol, 1.4 g) in water (20 mL) was added dropwise within 20 min. The mixture was stirred for further 40 minutes during which a white precipitate appeared. The methanol was evaporated under vacuum using a rotary evaporator, and the target compound was extracted from the aqueous phase with diethyl ether (2 × 200 mL). The extract was dried over Na_2SO_4 and evaporated to dryness. Yield of 5-acetyl-2-methyl-2-cyclohexen-1-one was 82% (810 mg, 5.33 mmol); elemental composition (HRMS): $C_9H_{12}O_2$, found (152.0845), calculated (152.0834). MS (EI): *m/z* (relative intensity) 109 (100), 43 (24), 81 (18), 79 (16), 95 (14), 108 (12), 53 (12), 82 (11). ^{1}H NMR ($CDCl_3$): C*H*$_3$−C═ (1.79, s, 3H), C*H*$_3$−C═O (2.21, s, 3H), −C*H*$_2$−CH−C*H*$_2$− (2.47−2.73, m, 4H), C*H*−C═O (3.07−3.17, m, 1H), C*H*═C (6.71, m, 1H). ^{13}C NMR (CDC_3): *C*H$_3$−C═ (15.6, DEPT +), *C*H$_2$−CH═ (27.4, DEPT −), *C*H$_3$−C═O (27.7, DEPT +), *C*H$_2$−C═O (39.3, DEPT −), *C*H−C═O (47.0, DEPT +), CH$_3$−C═ (135.7, DEPT 0), CH$_2$−*C*H═ (142.5, DEPT +), CH$_2$−*C*═O (197.4, DEPT 0), CH$_3$−C═O (207.7, DEPT 0).

5-(2,2-dideutero-1-methylethenyl)-2-methyl-2-cyclohexen-1-one (9,9-dideutero-carvone) and 5-(1-methyl-2-(^{13}*C)-ethenyl)-2-methyl-2-cyclohexen-1-one.* A suspension of either ^{13}C-methyl- or D_3-methyl-triphenyl-phosphonium bromide (*2*) (2.5 mmol, 1.0 g) in dry diethyl ether (100 mL, dried over NaH) was stirred under a nitrogen atmosphere, and a solution of butyllithium in hexane (1 mL, 2.5 mmol/mL) was added dropwise at room temperature. The deep orange mixture was stirred for an additional 10 min, and a solution of 5-acetyl-2-methyl-2-cyclohexen-1-one (2.5 mmol, 380 mg) in dry diethyl ether (10 mL) was then added dropwise. Stirring was continued for further 60 min, after which the reaction mixture was washed with a solution of KH_2PO_4 (3 mmol, 408 mg) in water (50 mL). The diethyl ether phase was dried over Na_2SO_4 and evaporated to dryness by means of a rotary evaporator at a water bath temperature of 37 °C. By HRGC the purity of the crude product was in the range of 50−70% with a major impurity of unreacted 5-acetyl-2-methyl-2-cyclohexen-1-one of approximately 20−40%. The crude reaction mixture was purified by column chromatography on a diol phase (Bakerbond Diol, 40 μm, pentane/diethyl ether gradient). Yield of purified 5-(2,2-dideutero-1-methylethenyl)-2-methyl-2-cyclohexen-1-one (9,9-dideutero-carvone) was 16% (62.5 mg, 0.41 mmol); purity 95% determined by HRGC; isotopic purity determined by MS(CI) 94% D_2, 5% 6 D_1, 1% D_0; elemental composition (HRMS): $C_{10}H_{12}D_2O$, found (152.1159), calculated (152.1165). MS (EI), *m/z* (relative intensity) 82 (100), 110 (50), 95 (40), 109 (36), 54 (35), 39 (32), 107 (28), 41 (20), 152 (18). Yield of purified 5-(1-methyl-2(^{13}C)-ethenyl)-2-methyl-2-cyclohexen-1-one (9-^{13}C-carvone) was 11% (42.3 mg, 0.28 mmol); purity 97% determined by HRGC; isotopic purity determined by MS(CI) 99%; elemental composition (HRMS): $C_9{}^{13}CH_{14}O$, found (151.1059), calculated (151.1075). MS (EI), *m/z* (relative intensity) 82(100), 109 (53), 94 (51), 54 (49), 108 (30), 107 (28), 39 (18), 41 (15), 151 (14).

NMR Spectroscopy. NMR spectra were recorded on a Bruker AM 360 (Bruker, Karlsruhe, Germany) in $CDCl_3$ with TMS as internal standard (δ = 0 ppm).

High-Resolution Gas Chromatography (HRGC)−Mass Spectrometry (MS). High-resolution gas chromatography was performed using a nonpolar capillary column (30 m × 0.25 mm i. d.; DB-5, J + W Scientific, Folsom, CA) in a model 5890 gas chromatograph (Hewlett Packard, Heilbronn, Germany). Sample injection was performed using the cold on-column technique. The volume injected ranged from 0.2 to 0.5 μL. The temperature during HRGC was held at 35 °C for 1 min and raised to 230 °C with a rate of 6 °C/min. Mass spectra were recorded on a Finnigan MAT 95S (Finnigan, Bremen, Germany) mass spectrometer in the electron ionization (EI) mode at 70 eV, in the chemical ionization (CI) mode at 115 eV with isobutane as reagent gas, and in high-resolution (HR) mode using perfluorokerosene as internal standard.

RESULTS AND DISCUSSION

Possible Mechanisms of Oxidative In Vivo Metabolism. It is generally accepted that metabolism of xenobiotics starts with either hydroxylation or epoxidation and, therefore, the following mechanisms seem possible to explain the formation of dihydrocarvonic acid (**M1**) and carvonic acid (**M2**) during oxidative in vivo metabolism of carvone. In pathway 1 (**Figure 1**) carvone epoxide would be the first intermediate, which after isomerization to the aldehyde and subsequent further oxidation would lead to **M1**. Consequently, **M2** would be a dehydrogenation product of **M1**. In pathway 1 the carboxy carbon atom of both the acids is derived from the methylene carbon atom of carvone. Pathway 2 (**Figure 1**) starts with hydroxylation at the methyl group of the isopropenyl side chain of carvone yielding an alcohol (*3*) which after further oxidation leads to **M2**. Hydrogenation of the latter will result in formation of **M1**. The carboxy carbon of the acids is now derived from the methyl carbon of the isopropenyl side chain of carvone. Finally, in pathway 3, a stabilized radical could be formed by hydrogen abstraction prior to oxidation leading to equivalency of the methyl and the methylene position yielding the acids **M1** and **M2** with a 50% scrambling of methyl- and methylene-derived carboxy groups.

For uroterpenolone (**M3**) also three possible pathways of formation can be postulated (**Figure 1**). The primary alcohol function of **M3** might stem from either the methylene group (pathway 1) or the methyl group (pathway 2) of the isopropenyl side chain of carvone. Additionally, there might also be a pathway operative in which scrambling occurs (pathway 3). In pathway 1 the hypothetical intermediate carvone epoxide is hydrated, whereas in pathways 2 and 3 hydration occurs at the double bond of 10-hydroxy-carvone, a compound that has been identified as a carvone metabolite in rabbits (*3*).

Synthesis of 9,9-Dideutero-carvone or 9-^{13}C-Carvone. On the basis of the postulated oxidation mechanisms (**Figure 1**) only the positions 9 and 10 of carvone are suitable for labeling. The following straightforward approach was developed to synthesize carvone labeled at the methylene position at carbon 9. The synthesis started from unlabeled carvone which was epoxygenated to yield 8,9-epoxy-carvone. The epoxide was hydrolyzed with diluted sulfuric acid in water/THF producing uroterpenolone which was cleaved with sodium metaperiodate yielding 5-acetyl-2-methyl-2-cyclohexen-1-one. From reaction of the latter with dideutero-methylene-triphenylphosphorane or with ^{13}C-methylene-triphenylphosphorane in a Wittig Reaction either 9,9-dideutero-carvone or 9-^{13}C-carvone was obtained (**Figure 2**).

Deuterium Distribution in M1 and M2 from 9,9-Dideutero-carvone. The deuterium-labeled carvone was metabolized in a MICA experiment, and the metabolites were obtained as

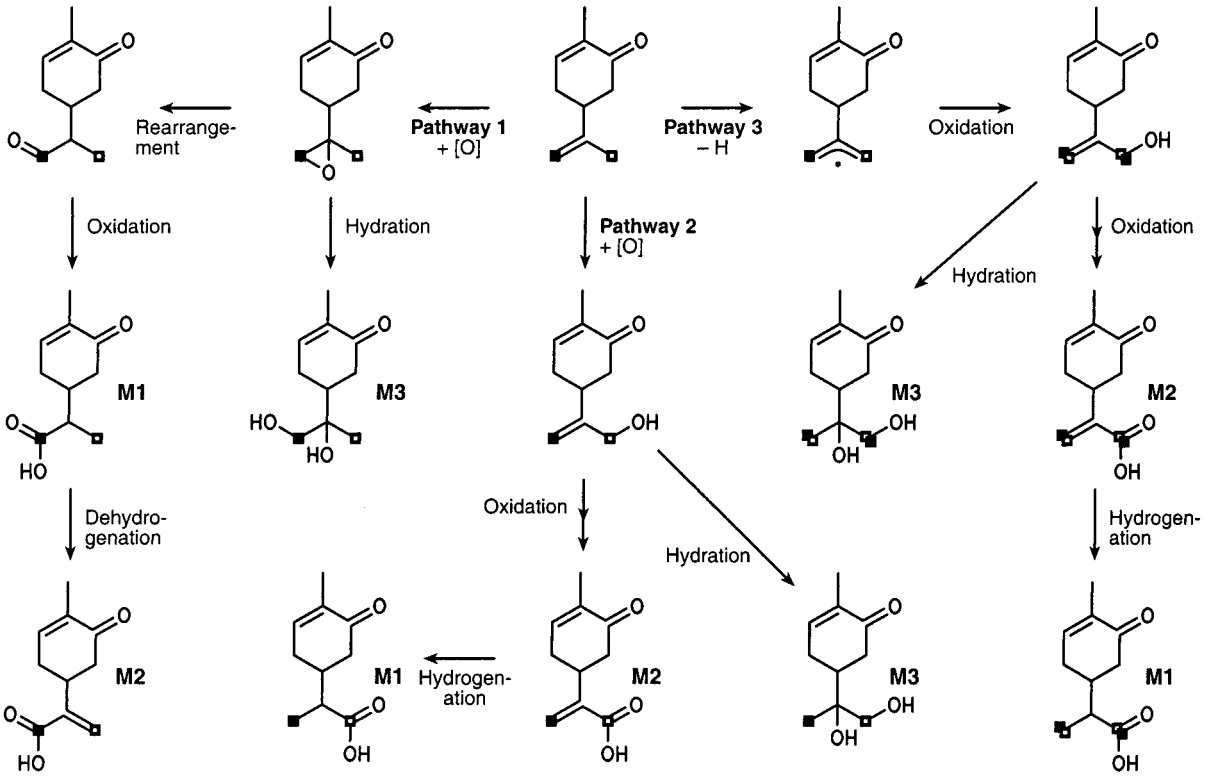

Figure 1. Possible mechanisms of oxidation of carvone during metabolism leading to dihydrocarvonic acid (**M1**), carvonic acid (**M2**), and uroterpenolone (**M3**). The filled square represents the methylene carbon, and the empty square represents the methyl carbon of the isopropenyl side chain of carvone.

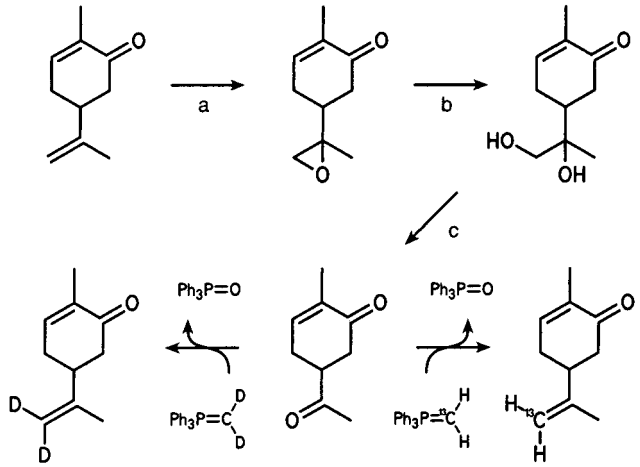

Figure 2. Synthesis of 9,9-dideutero-carvone and 9-^{13}C-carvone: (a) MCPBA in CH_2Cl_2 at room temperature; (b) H_2SO_4 in THF–H_2O (50:50, v/v) at room temperature; (c) $NaIO_4$ in MeOH–H_20 (50:50, v/v) at room temperature.

described recently for unlabeled carvone (*1*). The acidic fraction of an ethereal extract of the 24-h urine containing the metabolites was derivatized with iodoethane and further purified by HPLC on RP-18 material. The fractions containing the deuterated ethyl esters of **M1** and **M2** (**$D_{0\text{-}2}$-M1-ET** and **$D_{0\text{-}2}$-M2-ET**) were analyzed by high-resolution gas chromatography−mass spectrometry (HRGC−MS) in the chemical ionization (CI) mode to determine the amount of deuterium labeling. Because the most abundant isotopic ion and the mono-deuterated ion have the same mass, the measured intensities in all cases had to be corrected using the known natural isotopic distribution of carbon, namely 98.9% ^{12}C and 1.1% ^{13}C. The labeling distribution was calculated using the following method. Starting with the lowest ion *m*/*z* in the cluster analyzed, the amount of the naturally occurring $(m + 1)/z$ isotopic ion caused by ^{13}C was calculated as (amount of C-atoms) × 0.011 × (area of *m*/*z* ion). The value obtained was subtracted from the total area of $(m + 1)/z$ measured to obtain the value for the deuterium-labeled ion (**Tables 1** and **2**). The same results for both compounds were also obtained in the electron ionization (El) mode (data not shown). In this case for **$D_{0\text{-}2}$-M1-ET** the ions with *m*/*z* 102, 103, and 104 (**Figure 3**) resulting from McLafferty rearrangement (*4*, *5*) of the molecular ion and for **$D_{0\text{-}2}$-M2-ET** the molecular ions 208, 209, and 210 (**Figure 4**) were chosen for the calculations. The area values (**Tables 1** and **2**) are uncorrected for the incomplete labeling of 9,9-dideutero-carvone which was found to be 94% D_2, 5% D_1, and 1% D_0 by HRGC−MS in the CI mode, causing a negligible shift of the calculated values.

From the results of the deuterium labeling it is obvious that at least two different mechanisms of oxidation must be present, because the distribution of deuterium is not consistent with one of the three possible pathways alone. Since about half of **M1** carries only one deuterium, there must be the possibility of H−D exchange during metabolism. The existence of nearly 20% of mono-deuterated carvonic acid shows that the reaction between both acids has to be reversible to some extent, as from the possible pathways only nondeuterated or double-deuterated carvonic acid can be generated directly. However, labeling with ^{13}C is necessary to prove whether the undeuterated acids stem from complete deuterium exchange or from oxidation at the methylene position which, as a consequence, should also result in complete loss of deuterium. Therefore, in a second experiment, 9-^{13}C-carvone was administered in a MICA experiment.

Mass Spectrometric Fragmentation of M1-ET. To ensure proper interpretation of the ^{13}C labeling experiment, the mass spectrometric fragmentation of **M1-ET** had to be deduced by

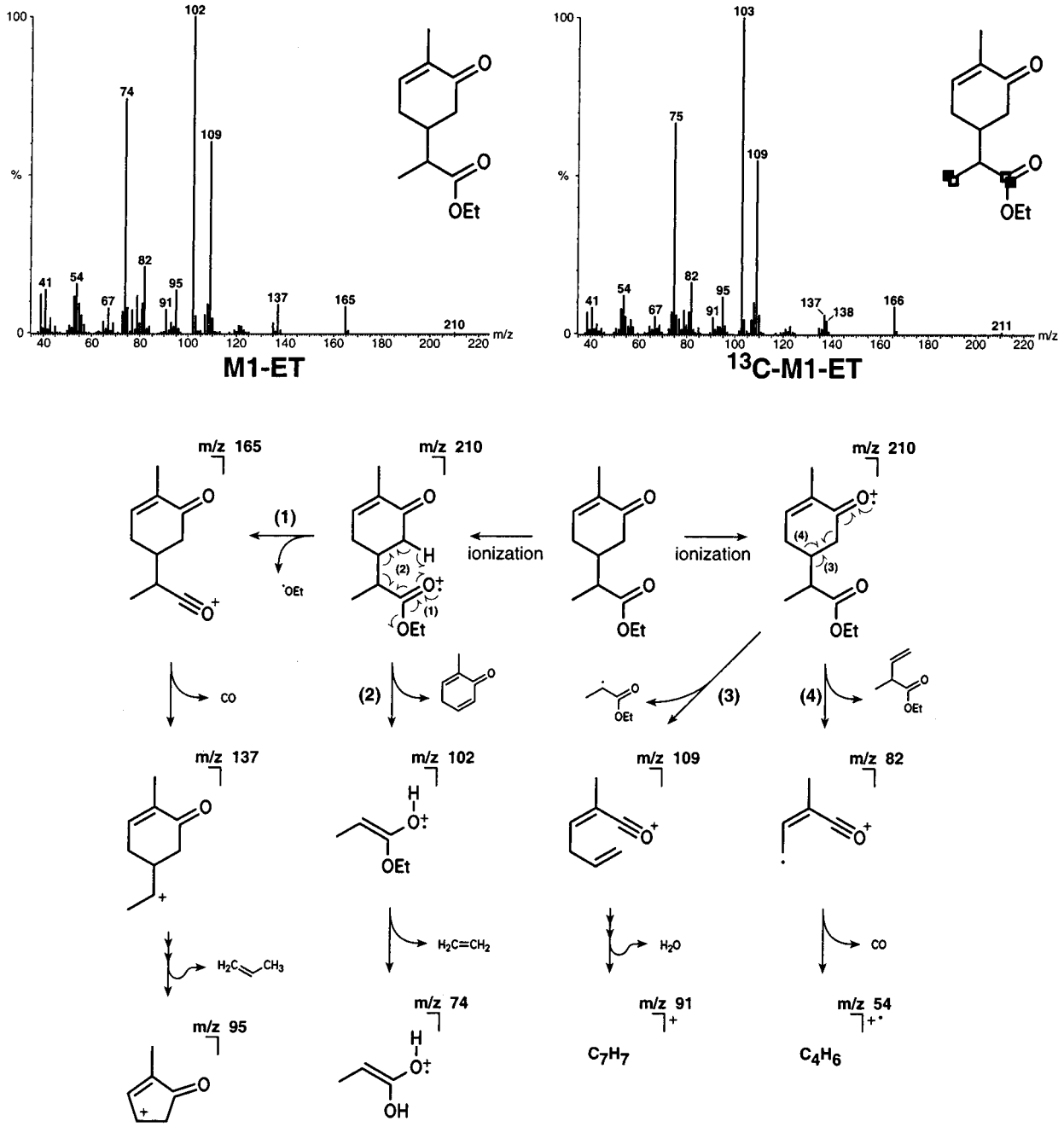

Figure 3. Mass spectra of unlabeled **M1-ET** and **^{13}C-M1-ET** and proposed mass spectrometric fragmentation of **M1-ET**. The filled square represents the ^{13}C label of the methylene carbon, and the empty square represents the methyl carbon of the isopropenyl side chain of carvone.

comparison of high-resolution mass spectrometry (HRMS) data of unlabeled **M1**, unlabeled **M1-ET**, **D$_{0\text{-}2}$-M1-ET**, and **^{13}C-M1-ET** (**Figure 3**, mass spectrum of unlabeled **M1** and **D$_{0\text{-}2}$-M1-ET** not shown). The ion with *m*/*z* 165 ($C_{10}H_{13}O_2$, all following *m*/*z* values and elemental compositions refer to unlabeled **M1-ET**) must be formed by α-cleavage of the molecular ion *m*/*z* 210 ($C_{12}H_{18}O_3$) by loss of an ethoxy radical. The ion *m*/*z* 137 ($C_9H_{13}O$) is formed by further loss of carbon monoxide from *m*/*z* 165 by charge-induced cleavage (**Figure 3**). The ions *m*/*z* 109 (C_7H_9O) and *m*/*z* 82 (C_5H_6O) are formed from the ring carbonyl mother ion and upon further fragmentation give *m*/*z* 91 (C_7H_7) and *m*/*z* 54 (C_4H_6). Ion *m*/*z* 95 (C_6H_7O) is most probably formed from ion *m*/*z* 137 by loss of propene. In the case of **^{13}C-M1-ET** ion *m*/*z* 95 carries no label and therefore its carbon atoms must stem from the ring, whereas, from the spectrum of **D$_{0-2}$-M1-ET** a considerable H−D exchange for ion *m*/*z* 95 was detected giving rise to about 50% *m*/*z* 96. Consequently, several hydrogen shifts involving the deuterium from the methyl group and a ring contraction have to take place during the reaction. Unfortunately, the base peak at *m*/*z* 102 formed by McLafferty rearrangement and the second most intensive signal at *m*/*z* 74 are not suitable for the determination of the labeling distribution. They contain both the methyl and the carboxy carbon of **M1** and thus are always totally shifted by one unit to *m*/*z* 103 and *m*/*z* 75, respectively. In conclusion, the ion with *m*/*z* 137, even though of minor relative intensity, is the only one suitable for successful determination of the ^{13}C distribution between the methyl and carboxy position.

^{13}C Distribution in M1 from 9-^{13}C-carvone. From the areas measured for the ions with *m*/*z* 137 and 138 for unlabeled **M1-ET**, a H-transfer cluster can be ruled out (**Table 3**). The area of ion with *m*/*z* 138 is completely generated by natural ^{13}C

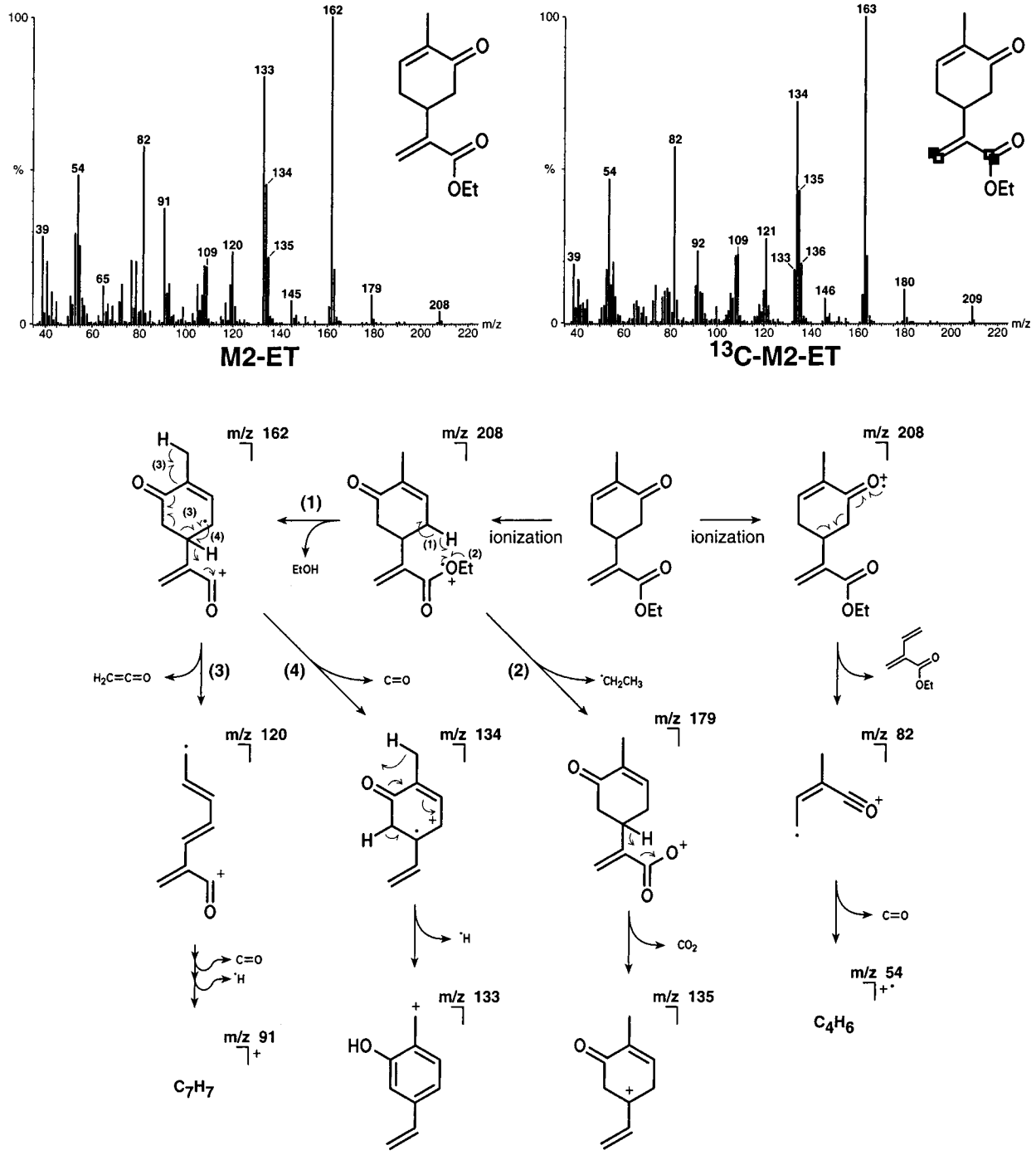

Figure 4. Mass spectra of unlabeled **M2-ET** and **^{13}C-M2-ET** and proposed mass spectrometric fragmentation of **M2-ET**. The filled square represents the ^{13}C label of the methylene carbon, and the empty square represents the methyl carbon of the isopropenyl side chain of carvone.

abundance in the remaining nine carbon atoms of ion *m*/*z* 137. The theoretical value calculated from (intensity of *m*/*z* 137) × (natural abundance of ^{13}C) × (number of carbon atoms in ion *m*/*z* 137) = $2.052 \times 10^6 \times 0.011 \times 9 = 0.207 \times 10^6$ is in good agreement with the measured value of 0.195×10^6. For **^{13}C-M1-ET** derived from 9-^{13}C-carvone this percentage of the area had to be subtracted from the measured value for the ion *m*/*z* 138 to obtain the amount for methyl-^{13}C labeled ion with also *m*/*z* 138 (**Table 3**). From these calculations, about 63% of the carboxy groups contain ^{13}C and thus stem from the methylene carbon, whereas about 37% do not contain the label and, therefore, must stem from the methyl carbon of the isopropenyl group of carvone.

Mass Spectrometric Fragmentation of M2-ET. The mass spectrometric fragmentation of **M2-ET** was deduced by comparison of high-resolution mass spectrometry (HRMS) data of unlabeled **M2**, unlabeled **M2-ET**, **$D_{0\text{-}2}$-M2-ET** and **^{13}C-M2-ET** (**Figure 4**, mass spectrum of unlabeled **M2** and **$D_{0\text{-}2}$-M2-ET** not shown). Even though **M2** is very closely related to **M1,** its double bond leads to a completely different mass spectrometric fragmentation. As can be seen from the comparison of the mass spectra of **M1-ET** (**Figure 3**) and **M2-ET** (**Figure 4**), because of the double bond in conjugation to the ester function, the McLafferty rearrangement to form a hypothetical ion *m*/*z* 100 does not take place. Overall, the presence of the double bond results in peaks with larger relative intensities at

Table 1. Areas below Mass Traces *m/z* 211, 212, 213, and 214 Determined for **$D_{0\text{-}2}$-M1-ET** in the Chemical Ionization Mode (CI) after Ingestion of 9,9-dideutero-carvone and Calculated Distribution for **D_0-M1-ET** (HH), **D_1-M1-ET** (HD), and **D_2-M1-ET** (DD)

m/z [a]	211		212		213		214	
area × 10^6 [b]	2.161		4.584		3.202		0.402 [g]	
HH : ^{13}CHH [c]	**2.161**	:	0.285					**23.7 ± 0.3%** [f]
HD : ^{13}CHD [d]			**4.299**	:	0.567			**47.5 ± 0.4%** [f]
DD : ^{13}CDD [e]					**2.635**	:	0.348 [g]	**28.8 ± 0.4%** [f]

[a] *m/z* Value of the ion. [b] Measured area units below the mass trace in the chemical ionization (CI) mode. [c] Calculated amount of the $[M + H]^+$ ion $C_{12}H_{19}O_3$ (HH, *m/z* 211) and $C_{11}{}^{13}CH_{18}O_3$ (^{13}CHH, *m/z* 212). [d] Calculated amount of the $[M + H]^+$ ion $C_{12}DH_{18}O_3$ (HD, *m/z* 212) and $C_{11}{}^{13}CDH_{17}O_3$ (^{13}CHD, *m/z* 213). [e] Calculated amount of the $[M + H]^+$ ion $C_{12}D_2H_{17}O_3$ (DD, *m/z* 213) and $C_{11}{}^{13}CD_2H_{16}O_3$ (^{13}CDD, *m/z* 214). [f] Mean %-values − deviation $n - 1$ weighting determined from 5 experiments. All area values in the table represent a single experiment and are used only to illustrate the calculation procedure. They do not necessarily produce the exact mean %-values. [g] Discrepancy results from instrumentation error and nonobservance of area produced by other isotopes.

Table 2. Areas below Mass Traces *m/z* 209, 210, 211, and 212 Determined for **$D_{0\text{-}2}$-M2-ET** in the Chemical Ionization Mode (CI) after Ingestion of 9,9-Dideutero-carvone, and Calculated Distribution for **D_0-M2-ET** (HH), **D_1-M2-ET** (HD), and **D_2-M2-ET** (DD)

m/z [a]	209		210		211		212	
area × 10^6 [b]	4.138		3.625		9.751		1.363 [g]	
HH : ^{13}CHH [c]	**4.138**	:	0.546					**24.9 ± 0.1%** [f]
HD : ^{13}CHD [d]			**3.079**	:	0.406			**18.7 ± 0.1%** [f]
DD : ^{13}CDD [e]					**9.345**	:	1.234 [g]	**56.4 ± 0.2%** [f]

[a] *m/z* Value of the ion. [b] Measured area units below the mass trace in the chemical ionization (CI) mode. [c] Calculated area of the $[M + H]^+$ ion $C_{12}H_{17}O_3$ (HH, *m/z* 209) and $C_{11}{}^{13}CH_{17}O_3$ (^{13}CHH, *m/z* 210). [d] Calculated area of the $[M + H]^+$ ion $C_{12}DH_{16}O_3$ (HD, *m/z* 210) and $C_{11}{}^{13}CDH_{16}O_3$ (^{13}CHD, *m/z* 211). [e] Calculated area of the $[M + H]^+$ ion $C_{12}D_2H_{15}O_3$ (DD, *m/z* 211) and $C_{11}{}^{13}CD_2H_{15}O_3$ (^{13}CDD, *m/z* 212). [f] Mean %-values − deviation $n - 1$ weighting determined from 5 experiments. All area values in the table represent a single experiment and are used only to illustrate the calculation procedure. They do not necessarily produce the exact mean %-values. [g] Discrepancy results from instrumentation error and nonobservance of area produced by other isotopes.

higher *m/z* values. From the quite intense molecular ion *m/z* 208 ($C_{12}H_{16}O_3$), formed by removal of an electron at the ring carbonyl oxygen, the ion series *m/z* 82 (C_5H_6O) and 54 (C_4H_6) is formed which is analogous to the fragmentation of **M1-ET.** Removal of an electron at the carbonyl of the ester function results in two different ion series. First, by removal of an ethyl radical the ion *m/z* 179 ($C_{10}H_{11}O_3$) is formed, resulting in an ion *m/z* 135 ($C_9H_{11}O$) after loss of carbon dioxide. Second, another ion series [(1) in **Figure 4**] is initiated by abstraction of a hydrogen from the cyclohexenone ring, resulting in the base peak *m/z* 162 ($C_{10}H_{10}O_2$) after loss of ethanol. Ion *m/z* 162 has a remarkable stability due to delocalization of both the radical and the positive charge. It decomposes further, losing carbon monoxide (*m/z* 134, $C_9H_{10}O$) and hydrogen (*m/z* 133, C_9H_9O). If ketene is lost prior to carbon monoxide an analogous ion series with *m/z* 120 (C_8H_8O), *m/z* 92 (C_7H_8, not shown in **Figure 4**), and *m/z* 91 (C_7H_7) results. The high intensity, and thus stability, of ion *m/z* 133 results from its aromatic character and the stabilization of the charge by the electron-donating +M effect of the hydroxy and the ethenyl group. As this ion is the one with the lowest mass in the H cluster *m/z* 133, 134, 135, and it carries only the methylene position of **M2**, it is most suitable for determining the distribution of ^{13}C in **^{13}C-M2-ET**.

Table 3. Areas below the Mass Traces *m/z* 137 and 138 Determined for **M1-ET** Derived from Unlabeled Carvone and **^{13}C-M1-ET** Derived from 9-^{13}C-carvone and Calculated Distribution for **^{13}C-M1-ET**

m/z [a]	137		138	
elemental composition	$C_9H_{13}O$		$C_8{}^{13}CH_{13}O$	
unl.-M1-ET area × 10^6 [b]	2.052		0.195 [d]	
^{13}C-M1-ET area × 10^6 [c]	15.462		10.470 [e]	
carboxy-labeled M1	**15.462**	:	1.530 [f]	**63.2 ± 0.2%** [g]
α-methyl-labeled M1			**8.940**	**36.8 ± 0.2%** [g]

[a] *m/z* Value of the ion. [b] Measured area units below the mass trace in the electron ionization (EI) mode for unlabeled **M1-ET.** [c] Measured area units below the mass trace in the electron ionization (EI) mode for **^{13}C-M1-ET.** [d] Area resulting from natural abundance of ^{13}C in ion *m/z* 137. [e] Area resulting from natural abundance of ^{13}C in ion *m/z* 137 and from singly ^{13}C labeled ion $C_8{}^{13}CH_9O$ where all remaining carbon atoms are ^{12}C. [f] Theoretical area resulting from natural abundance of ^{13}C in ion *m/z* 137. [g] Mean %-values − deviation $n - 1$ weighting determined from 5 experiments. All area values in the table represent a single experiment and are used only to illustrate the calculation procedure. They do not necessarily produce the exact mean %-values.

Table 4. Areas below the Mass Traces *m/z* 133 and 134 Determined for **M2-ET** Derived from Unlabeled Carvone and **^{13}C-M2-ET** Derived from 9-^{13}C-carvone and Calculated Distribution for **^{13}C-M2-ET**

m/z [a]	133		134	
elemental composition	C_9H_9O		$C_9H_{10}O + C_8{}^{13}CH_9O$	
unl.-M2-ET area × 10^6 [b]	1.844		1.038 [d]	
^{13}C-M2-ET area × 10^6 [c]	2.093		8.649 [e]	
carboxy-labeled M2	**2.093**	:	1.178 [f]	**22.2 ± 0.4%** [g]
α-methylene-labeled M2			**7.471**	**77.8 ± 0.4%** [g]

[a] *m/z* Value of the ion. [b] Measured area units below the mass trace in the electron ionization (EI) mode for unlabeled **M2-ET.** [c] Measured area units below the mass trace in the electron ionization (EI) mode for **^{13}C-M2-ET.** [d] Area resulting from natural abundance of ^{13}C in ion *m/z* 133 and from ion $C_9H_{10}O$ with *m/z* 134. [e] Area resulting from natural abundance of ^{13}C in ion *m/z* 133, from ion $C_9H_{10}O$ with *m/z* 134, and from singly ^{13}C labeled ion $C_8{}^{13}CH_9O$ where all remaining carbon atoms are ^{12}C. [f] Theoretical area resulting from natural abundance of ^{13}C in ion *m/z* 133 and from ion $C_9H_{10}O$ with *m/z* 134 [g] Mean %-values − deviation $n - 1$ weighting determined from 5 experiments. All area values in the table represent a single experiment and are used only to illustrate the calculation procedure. They do not necessarily produce the exact mean %-values.

^{13}C Distribution in M2 from 9-^{13}C-carvone. From the measured values of the cluster 133, 134 in unlabeled **M2-ET** the distribution of the label in **^{13}C-M2-ET** was calculated as follows (all area values from **Table 4**). For **^{13}C-M2-ET** an amount of 2.093×10^6 area units for *m/z* 133 (C_9H_9O) would result in an area of $2.093 \times 10^6 \times (1.038 \times 10^6/1.844 \times 10^6) = 1.178 \times 10^6$ for the expected amount of *m/z* 134 ($C_9H_{10}O$ plus $C_8{}^{13}CH_9O$ resulting from natural abundance). This amount would leave an area of $8.649 \times 10^6 - 1.178 \times 10^6 = 7.471 \times 10^6$ for the ion *m/z* 134 ($C_8{}^{13}CH_9O$) with the ^{13}C label at the methylene position. Consequently, about 78% of the ^{13}C label in **M2** are still at the methylene position, whereas the remaining 22% have to be located at the carboxy group forming unlabeled ion *m/z* 133 in **^{13}C-M2-ET**.

Mass Spectrometric Fragmentation of M3-TMS and Deuterium Distribution in M3 from 9,9-Dideutero-carvone. From the shift of *m/z* 147 in undeuterated trimethylsilylated **M3** (**M3-TMS**) to *m/z* 149 in **D_2-M3-TMS** (**Figure 5**) it could be concluded that both deuterium atoms were still present in **M3** and no deuterium exchange took place during metabolism. From MS-EI the position was determined according to the mass spectrometric fragmentation of **M3-TMS** (**Figure 5**), which was deduced from HRMS. Ion m/z 153 ($C_9H_{13}O_2$) being present in

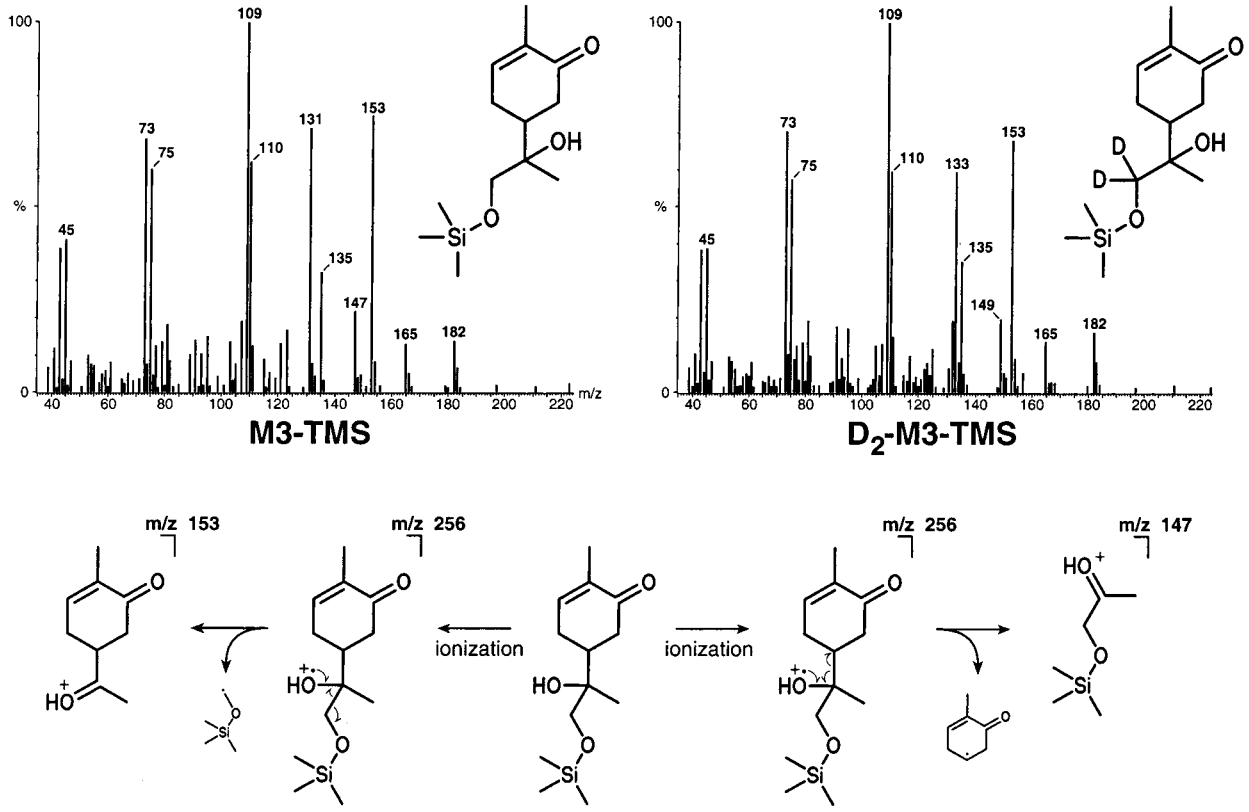

Figure 5. Mass spectra of unlabeled **M3-TMS** and **D_2-M3-TMS** and proposed mass spectrometric formation of relevant ions useful for the determination of the deuterium labeling in **M3-TMS**.

the mass spectrum of **M3-TMS** and **D_2-M3-TMS** with unchanged intensity proves that the methyl group does not carry deuterium and, therefore, stems from the unlabeled methyl group of carvone. Ion *m*/*z* 147 ($C_6H_{15}O_2Si$) in the mass spectrum of unlabeled **M3-TMS** is completely shifted to *m*/*z* 149 in **D_2-M3-TMS** proving the presence of both deuterium labels in **M3** at the HO−C**H_2**− position. The ^{13}C labeling experiment (data not shown) fully confirmed the results obtained by the deuterium labeling.

It is remarkable that the ^{13}C distribution for **M2**, where about 22% of the label was located at the carboxy group and 78% was located at the methylene group, is nearly the opposite of the distribution found in **M1**, where about 64% of the label was located at the carboxy group and only 36% was located at the methyl group. Therefore, even though **M1** and **M2** are closely related from a structural point of view, neither **M2** is the direct precursor for **M1**, nor is **M1** the precursor for **M2**. Consequently, both acids are primarily generated by independent pathways.

From the results, the symmetrical-radical mechanism (pathway 3 in **Figure 1**) cannot be completely ruled out, but because of the following points it has to be considered unlikely or of minor importance. The presence of 29% **D_2-M1** clearly shows that reduction of **D_2-M2** without loss of deuterium is possible, since there is no other formation pathway for **D_2-M1**. As a consequence, the presence of **D_1-M2** proves, that also the reverse reaction, that is the dehydrogenation of **D_2-M1**, is possible to some extent. The same reaction will also generate **D_0-M2** from both **D_0-M1** or **D_1-M1** being labeled at the carboxy-group. Therefore, the amount of 22% **M2** labeled at the carboxy group can be explained without the symmetrical-radical mechanism (pathway 3 in **Figure 1**).

More importantly, the combined results of D_2 and ^{13}C labeling for **M1** prove a hydride shift during the process of oxidation. If a methylene group would be oxidized to a carboxy group without a hydride shift, more than 63% of **M1** (**Table 3**) would be expected not to carry any deuterium. However, only about 24% of **M1** (**Table 1**) was found undeuterated and nearly 48% was found mono-deuterated. This observation can be explained only by the so-called NIH shift, which occurs in vivo during enzymatic hydroxylation of aromatic compounds (*6*). In nonenzymatic model experiments the NIH shift was observed during acid-catalyzed rearrangements of deuterated epoxides (*7*) or 5,6-dihydroxy-cyclohexa-1,3-dienes (*8*) synthesized from labeled aromatic compounds. Probably the most common example of a NIH shift is found in the biosynthesis of tyrosine from phenylalanine (*6*, *9*) where the 4-hydrogen of the phenyl ring of phenylalanine is later partially found in the 3-position of tyrosine. There is evidence for the involvement of an epoxide, which in one case (*10*) was even isolated, or for a cationic (*11*) or even radical intermediate (*12*). The mechanistic situation becomes even more complicated because in two flavine monooxygenase model systems the NIH shift could not be detected (*13*) indicating the possibility of a different mechanism. However, to our knowledge a NIH shift has never been found in connection with nonaromatic compounds and, generally, it is assumed that aliphatic epoxides are either reduced to alcohols or hydrated forming a 1,2-diol. Therefore, this work reports the first NIH shift observed on a nonaromatic compound introducing the term "nonaromatic" NIH shift. As it is yet unclear whether epoxides are intermediates in all cases, the term "epoxide-equivalent" will be used in the following text.

It is noteworthy that the postulated product of the "nonaromatic" NIH shift, 8,9-dihydro-carvonaldehyde, will lose some of the shifted hydride prior to further oxidation due to partial enolization. This is very well reflected by the high percentage (23% of total **M1**, **Figure 6**) of carboxy-labeled **M1** not containing any original hydrogens from carvone.

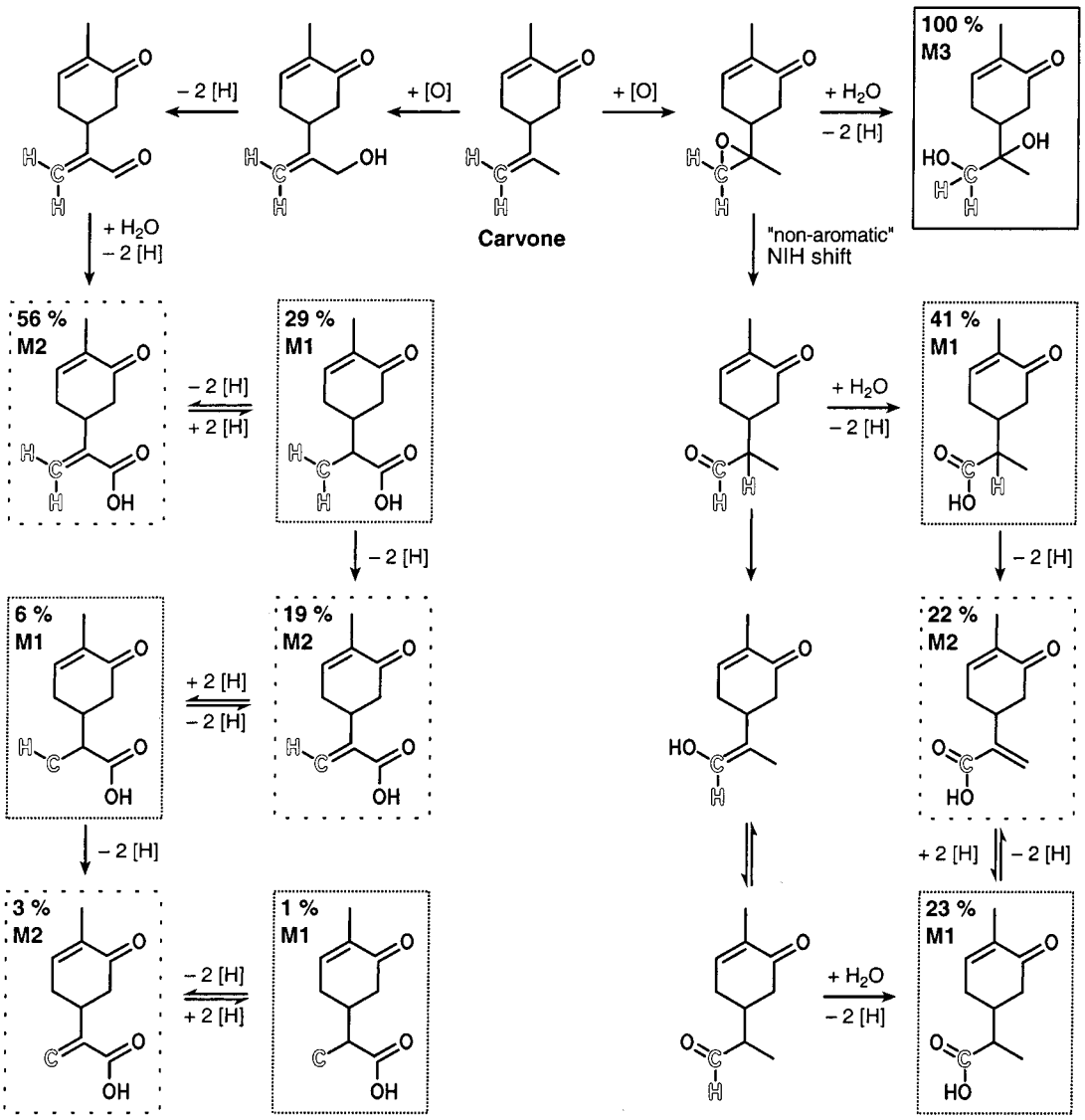

Figure 6. Formation of **M1**, **M2**, and **M3** during in vivo metabolism of carvone in humans. The outlined Hs represent the original hydrogen atoms of carvone and the outlined Cs represent the methylene carbon of carvone. Percentage values for each metabolite calculated from the combined results of the D- and ^{13}C-labeling experiments.

From the results obtained for **M3** it is obvious that it is generated by pathway 1 in **Figure 2** because the deuterium labels were found at the primary alcohol function. In this case the usual fate of an aliphatic epoxide-equivalent is observed resulting in 1,2-diol formation after hydration. To conclude, the following pathways lead to the major oxygenated in vivo metabolites of carvone in humans (**Figure 6**). Carvone is partially transformed to a carvone epoxide-equivalent which is converted to **M1** by rearrangement followed by further oxidation. In another reaction sequence the epoxide-equivalent can also be hydrolyzed to the 1,2-diol **M3.** Carvone is also oxidized at the methyl carbon of the isopropenyl side chain. Most probably 10-hydroxy-carvone is an intermediate, being rapidly and completely further oxidized to **M2**. The alcohol, 10-hydroxy-carvone, was identified in rabbits (*2*) but could not be detected in MICA experiments (*1*). The conversion of **M1** to **M2** by dehydrogenation and vice versa of **M2** to **M1** by hydrogenation is possible but obviously slower than conjugation or excretion. If the opposite were the case, the ^{13}C label should be equally distributed between both positions and, additionally, the deuterium label should be more or less completely removed; neither was found to be the case.

ACKNOWLEDGMENT

I gratefully acknowledge the support of Ines Otte and Julius Schönauer for mass spectrometry.

LITERATURE CITED

(1) Engel, W. In vivo studies on the metabolism of the monoterpenes *S*-(+)- and *R*-(−)-carvone in humans using the metabolism of ingestion-correlated amounts (MICA) approach. *J. Agric. Food Chem.* **2001**, *49*, 4069−4075.

(2) Gajewski, J. J.; Peterson, K. B.; Kagel, J. R.; Huang, Y. C. J. Transition-state structure variation in the Diels−Alder reaction from secondary deuterium kinetic isotope effects. The reaction of nearly symmetrical dienes and dienophiles is nearly synchronous. *J. Am. Chem. Soc.* **1989**, *111*, 9078−9081.

(3) Ishida, T.; Toyota, M.; Asakawa, Y. Terpenoid biotransformation in mammals. V. Metabolism of (+)-citronellal, (±)-7-hydroxycitronellal, citral, (−)-perillaldehyde, (−)-myrtenal, cuminaldehyde, thujone, and (±)-carvone in rabbits. *Xenobiotica* **1989**, *19*, 843−855.

(4) McLafferty, F. W. Mass spectrometric analysis. Molecular rearrangements. *Anal. Chem.* **1959**, *31*, 82−87.

(5) Kingston, D. G. I.; Bursey, J. T.; Bursey, M. M. Intramolecular hydrogen transfer in mass spectra. II. McLafferty rearrangement and related reactions. *Chem. Rev.* **1974**, *74*, 215−242.
(6) Guroff, G.; Daly, J. W.; Jerina, D. M.; Renson, J.; Witkop, B.; Udenfried, S. Hydroxylation-induced migration. NIH shift. *Science* **1967**, *157*, 1527−1530.
(7) Jerina, D. M.; Daly, J. W.; Witkop, B. The role of arene oxide-oxepin systems in the metabolism of aromatic substrates. II. Synthesis of 3,4-toluene-4-d oxide and subsequent "NIH shift" to 4-hydroxytoluene-3-d. *J. Am. Chem. Soc.* **1968**, *90*, 6523−6525.
(8) Jerina, D. M.; Daly, J. W.; Witkop, B. Deuterium migration during the acid-catalyzed dehydration of 6-deuterio-5,6-dihydroxy-3-chloro-1, 3- cyclohexadiene, a nonenzymatic model for the NIH shift. *J. Am. Chem. Soc.* **1967**, *89*, 5488−5489.
(9) Lehmann, W. D.; Heinrich, H. C. The NIH-shift in the in vivo hydroxylation of ring-deuterated L-phenylalanine in man. *Arch. Biochem. Biophys.* **1986**, *250*, 180−185.
(10) Boyd, D. R.; Sharma, N. D.; Harrison J. S.; Hamilton, J. T. G. McRoberts, W. C.; Harper, D. B. Isolation of a stable benzene oxide from a fungal biotransformation and evidence for an "NIH shift" of the carbomethoxy group during hydroxylation of methyl benzoates. *Chem. Commun.* **2000**, *16*, 1481−1482.
(11) Vanelli, T.; Hooper, A. B. NIH shift in the hydroxylation of aromatic compounds by the ammonia-oxidizing bacterium *Nitrosomonas europaea*. Evidence against an arene oxide intermediate. *Biochemistry* **1995**, *34*, 11743−11749.
(12) Bhatt, M. V.; Periasamy, M. Rearrangements in the cerium(IV) and manganese(III) oxidations of substituted naphthalenes and the NIH shift mechanism. *Tetrahedron* **1994**, *50*, 3575−3586.
(13) Smith, J. R. L.; Jerina, D. M.; Kaufman, S.; Milstein, S. Aromatic hydroxylation mediated by flavin autoxidation. Lack of the NIH shift. *J. Chem. Soc., Chem. Commun.* **1975**, *21*, 881−882.

Received for review September 10, 2001. Revised manuscript received December 14, 2001. Accepted December 18, 2001. I thank the Deutsche Forschungsanstalt für Lebensmittelchemie for financial support of this work.

JF011199H